Supplementary Information

Iron-containing POM-Based Hybrid Compound as Heterogeneous Catalyst for One-Step Hydroxylation of Benzene to Phenol

Si-Man Li,[a] Ji-Lei Wang,[a] Jiu-Lin Zhou,[a] Xin-Ying Xiang,[a] Ya-Ting Yu,[a] Qun Chen,[a] Hua Mei*[a] and Yan Xu*[a,b]

a. College of Chemical Engineering, State Key Laboratory of Materials-Oriented Chemical Engineering, Nanjing Tech University, Nanjing 211816, P. R. China.
b. State Key Laboratory of Coordination Chemistry, School of Chemistry and Chemical Engineering, Nanjing University, Nanjing 210023, P. R. China.

Table of Contents

Experimental section

Instruments

$H_6PMo_9V_3O_{40}·32.5H_2O$ was prepared according to the method provided in reference[38]. All other chemicals were used commercially available chemicals without further purification. The content of the samples (C, H and N) was through the use of PerkinElmer 2400 element analyzer measurement. Compound PXRD analysis was conducted on Smartlab TM 9 KW diffractometer, using monochromatized Cu-Kα (λ = 0.15418 nm) radiation ranging from 5 to 50°. FT-IR spectra (4000-400 cm−1) were acquired by using a Nicolet Impact 410 FT-IR spectrometer. Thermogravimetric (TG) measurement was performed using a Diamond thermogravimetric analyzer under the environment of nitrogen (25 to 1000 °C, 10 °C min-1). X-ray photoelectron spectroscopy (XPS) analysis was performed with AXIS SUPRA from Japan. The F-4600 FL spectrophotometer was used to obtain photoluminescence (PL) spectra at room temperature with an excitation wavelength of 340 nm. Electron paramagnetic resonance (EPR) spectra were taken on Bruker EMX-10/12 electron spin resonance spectrometer at room temperature.

Synthsis of $H_6PMo_9V_3O_{40}·32.5H_2O$.

MoO_3 (12.96 g, 0.090 mol) and V_2O_5 (2.73 g, 0.015 mol) with deionized water (250 mL) were heated to 120 °C under vigorous stirring in a flask equipped with a condenser and a magnetic stirrer. H_3PO_4 (85%, 1.15 g, 0.010 mol) was added dropwise to 10 mL of water, which was then slowly added dropwise to the above mixture and heated at 120 °C for 24 h to form an orange-red solution. The solution was cooled to room temperature and dried under vacuum at 50 °C for 24 h to obtain an orange fine powder. The powdered solid was recrystallized to obtain the final product.

Benzene hydroxylation to phenol

The benzene conversion and phenol yields were calculated using the following formulas.

$$Conversion\ (benzene) = 1 - (\frac{remained\ benzene\ concentration}{initial\ benzene\ concentration}) \times 100\%$$

$$Yield\ (phenol) = \frac{produced\ phenol\ concentration}{initial\ benzene\ concentration} \times 100\%$$

$$Selectivity = \frac{Yield\ (phenol)}{Conversion\ (benzene)} \times 100\%$$

$$Utilization(H_2O_2) = \frac{produced\ phenol\ concentration}{initial\ H_2O_2\ concentration} \times 100\%$$

X-ray crystallography

Single-crystal X-ray diffraction of the compounds was carried out and data were collected on a Bruker Apex II CCD diffractometer with graphite monochromatic Mo–K_α radiation (λ =0.71073 Å) as the radiation source at 296 K. Hereafter, the crystal structures were resolved by direct methods and refined on F2 by full-matrix least-squares methods via SHELX-2018/3 and the Olex 2 program package. Moreover, the anisotropic thermal parameters were applied to refine all the non-H atoms. Hydrogen atoms on organic molecules in the complexes were obtained by theoretical hydrogenation. Table 1 shows the crystallographic data for **Fe_2-$PMo_{11}V_3$**, while their corresponding bond lengths and angles are displayed in Tables S1 and S2.

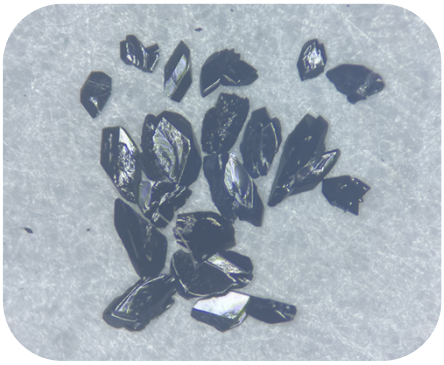

Figure S1 The image of **Fe_2-$PMo_{11}V_3$** under optical microscope.

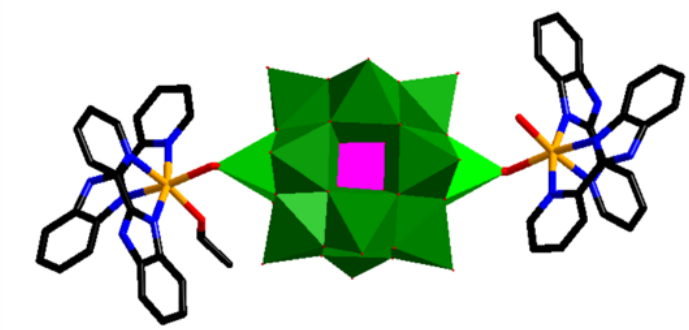

Figure S2 Polyhedral diagram of **Fe_2-$PMo_{11}V_3$**.

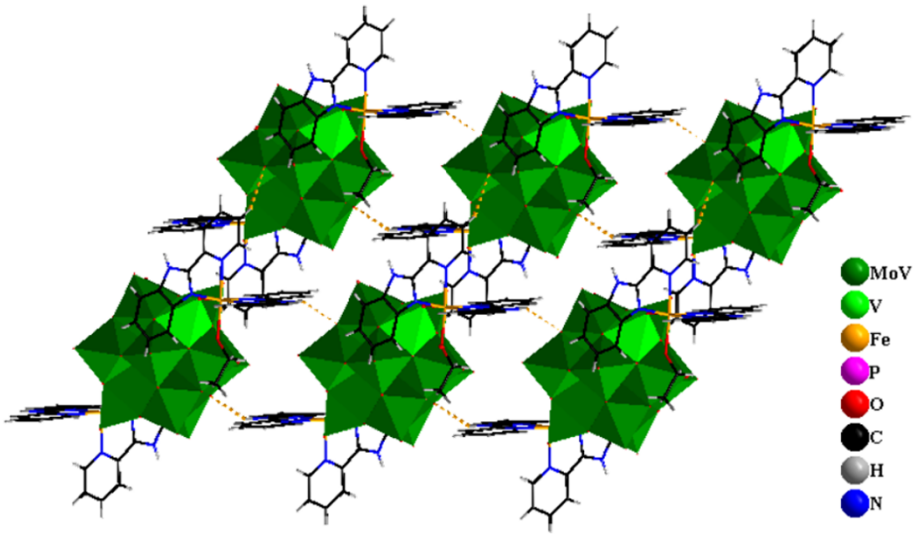

Figure S3 The 2D layer structure of **Fe_2-$PMo_{11}V_3$**, and the hydrogen bonding interactions in **Fe_2-$PMo_{11}V_3$**. The crystallization water molecules are omitted for clarity.

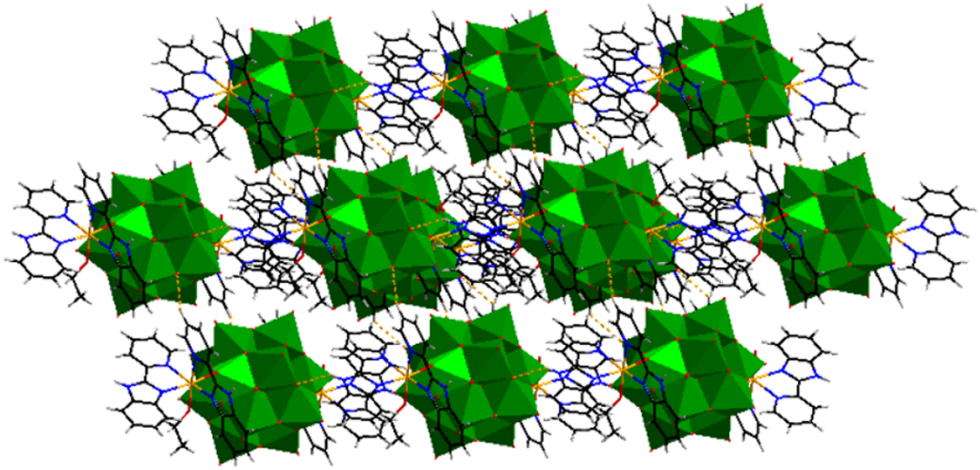

Figure S4 The 3D supramolecular structure of **Fe_2-$PMo_{11}V_3$** through the hydrogen bonding interactions.

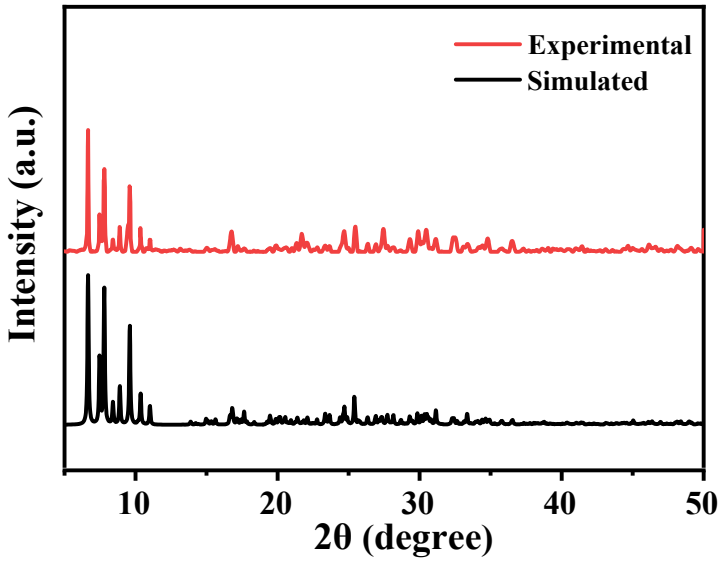

Figure S5 The simulated (black) and experimental (red) power X-ray diffraction patterns of **Fe_2-$PMo_{11}V_3$**.

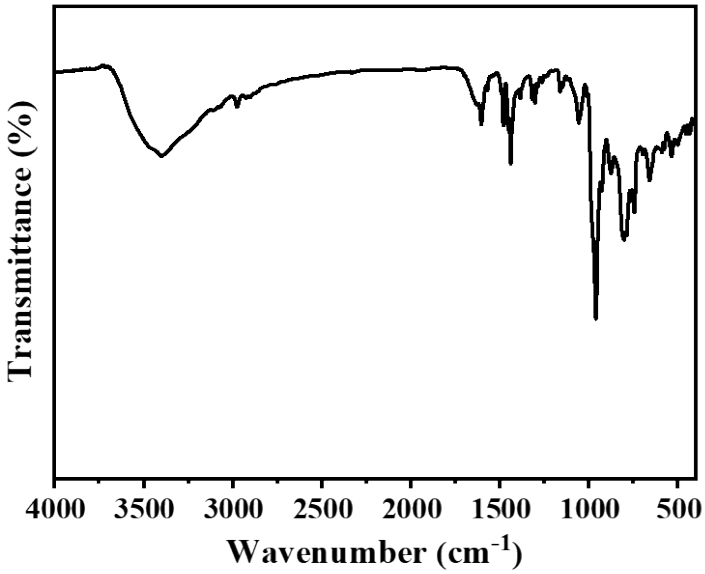

Figure S6 FT-IR spectrum of **Fe_2-$PMo_{11}V_3$**.

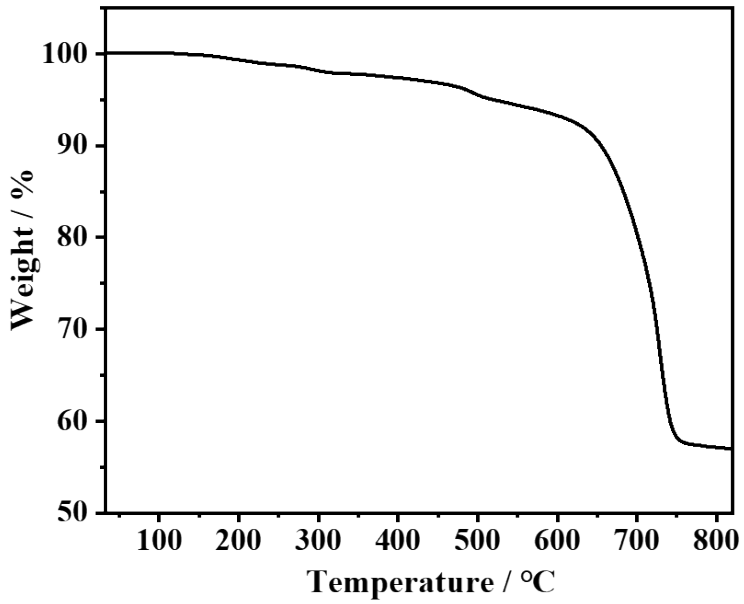

Figure S7 The TG curves of **Fe_2-$PMo_{11}V_3$**.

In the first part, below 300 °C, the weight loss of 2.63% (calc. 2.67 %) was considered as the loss of one lattice water molecule, one ligated ethanol molecule and one ligated water molecule. In the temperature range of 300 to 650 °C, 6.89% (calc. 6.75 %) of the loss was attributed to the removal of a pyim ligand. When the temperature exceeds 650 °C, the other pyim molecules are gradually removed and the whole M-O framework starts to collapse as the temperature increases further.

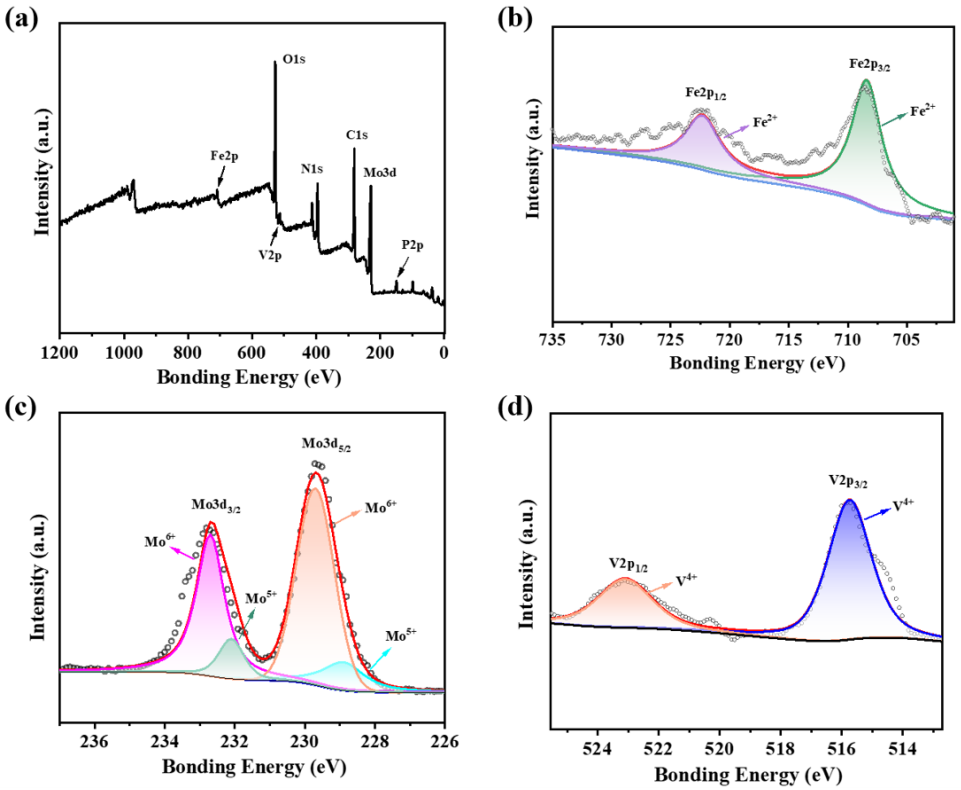

Figure S8 XPS spectra of (a) survey spectra, (b) Fe 2p, (c) Mo 3d, (d) V 2p, for **Fe_2-$PMo_{11}V_3$**.

As shown in the survey XPS spectrum (Figure S8a), the photoelectron peak is detected for O, V, Mo, N, C, Fe, P, which constituted the catalyst. The Fe2p energy spectrum exhibits two classical peaks attributed to Fe^{2+} at 722.7 and 708.7 eV (Figure S8b).[1] The high resolution of Mo3d is presented in Figure S8c, the characteristic binding energies of 232.7 eV and 229.8 eV belong to Mo^{6+}, while 232.2 eV and 228.9 eV belong to Mo^{5+}.[2] Furthermore, the ratio of the peak areas of $Mo^{VI}3d_{5/2}$ to $Mo^{V}3d_{5/2}$ in XPS is approximately 9:2, indicating a 9:2 ratio of Mo^{6+} to Mo^{5+}, which is in good agreement with the theoretical calculation results. As illustrated in Figure S8d, the energy spectrum of V2p shows two peaks at 515.8 eV and 523.0 eV, which are attributed to V^{4+}.[3]

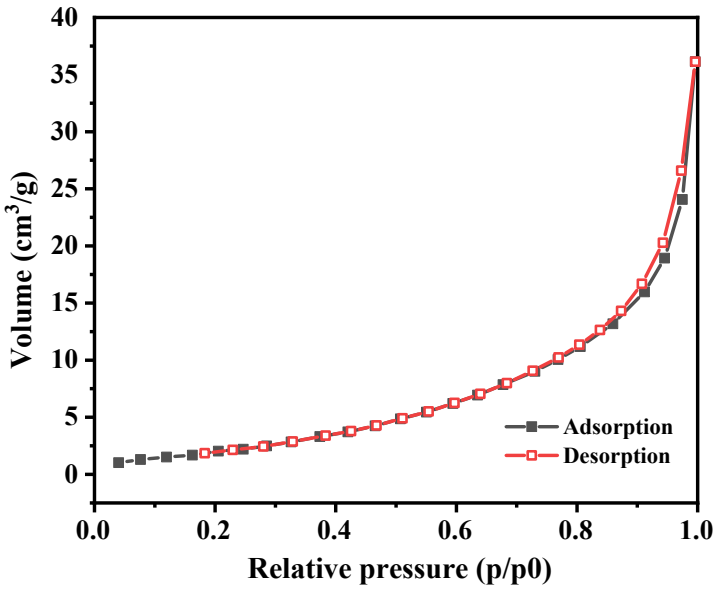

Figure S9 Nitrogen adsorption–desorption isotherm of **Fe_2-$PMo_{11}V_3$**.

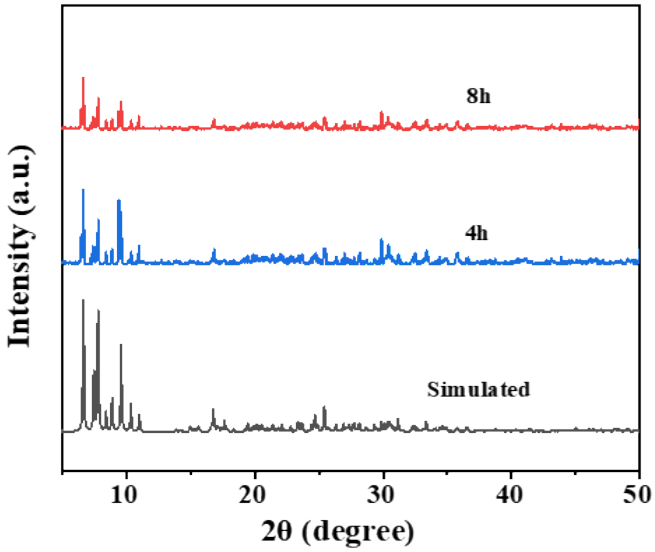

Figure S10 PXRD patterns of **Fe_2-$PMo_{11}V_3$** immersed in acetonitrile at different durations (4 h, 8 h).

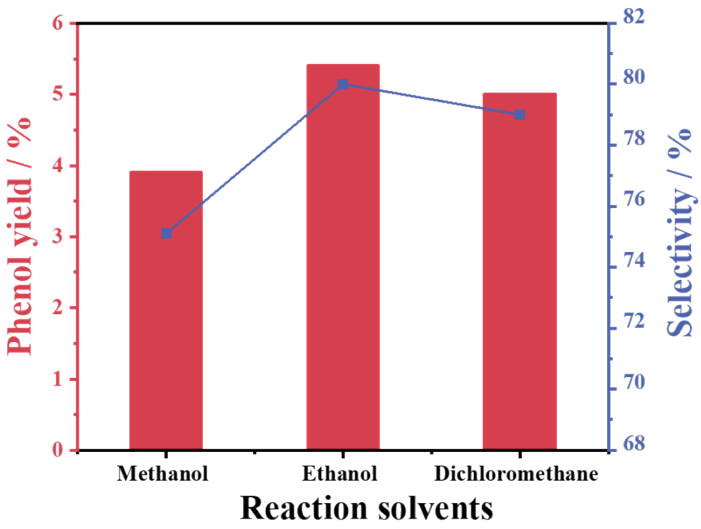

Figure S11 Effect of different reaction solvents in the hydroxylation of benzene. Reaction conditions: benzene (10 mmol), acetic acid (1 mL), methanol (5 mL), H_2O_2 (30 mmol), 60 °C, 6 h.

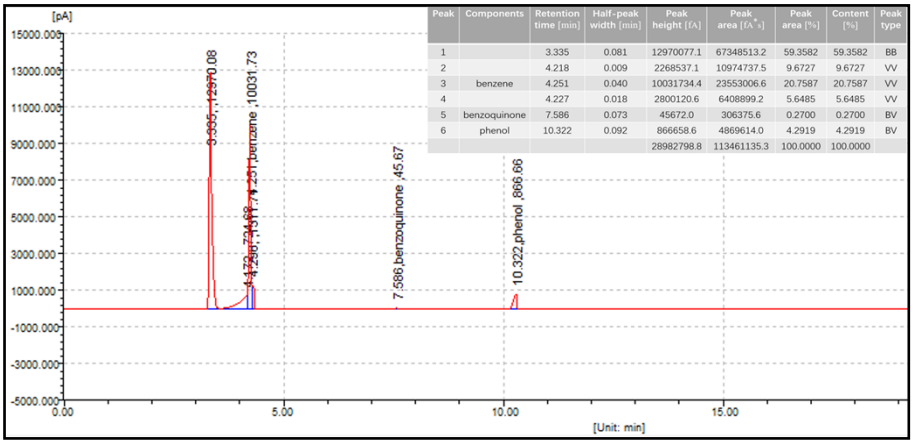

Peak	Components	Retention time [min]	Half-peak width [min]	Peak height [fA]	Peak area [fA*s]	Peak area [%]	Content [%]	Peak type
1		3.335	0.081	12970077.1	67348513.2	59.3582	59.3582	BB
2		4.218	0.009	2268537.1	10974737.5	9.6727	9.6727	VV
3	benzene	4.251	0.040	10031734.4	23553006.6	20.7587	20.7587	VV
4		4.227	0.018	2800120.6	6408899.2	5.6485	5.6485	VV
5	benzoquinone	7.586	0.073	45672.0	306375.6	0.2700	0.2700	BV
6	phenol	10.322	0.092	866658.6	4869614.0	4.2919	4.2919	BV
				28982798.8	113461135.3	100.0000	100.0000	

Figure S12 The GC profile under optimal reaction conditions.

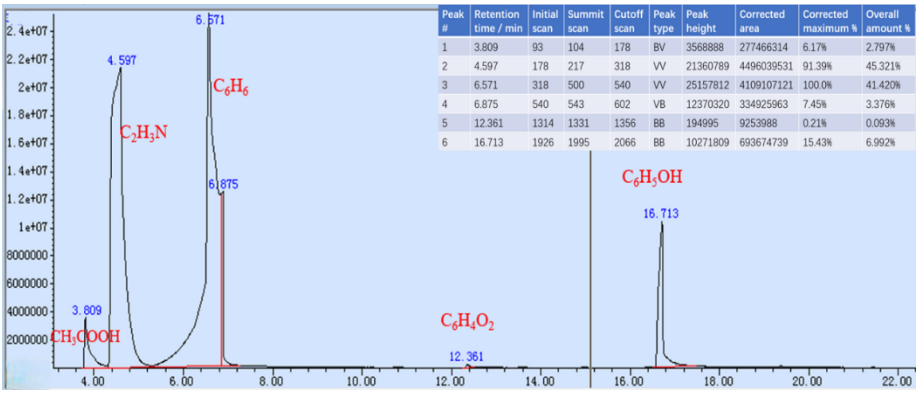

Peak #	Retention time / min	Initial scan	Summit scan	Cutoff scan	Peak type	Peak height	Corrected area	Corrected maximum %	Overall amount %
1	3.809	93	104	178	BV	3568888	277466314	6.17%	2.797%
2	4.597	178	217	318	VV	21360789	4496039531	91.39%	45.321%
3	6.571	318	500	540	VV	25157812	4109107121	100.0%	41.420%
4	6.875	540	543	602	VB	12370320	334925963	7.45%	3.376%
5	12.361	1314	1331	1356	BB	194995	9253988	0.21%	0.093%
6	16.713	1926	1995	2066	BB	10271809	693674739	15.43%	6.992%

Figure S13 The GC-MS trace.

Table S1 The bond lengths (Å) of main metal atoms for **Fe_2-$PMo_{11}V_3$**.

Mo(1)-O(13)	1.655(6)	Mo(4)-O(21)	2.500(10)
Mo(1)-O(14)	1.809(6)	Mo(5)-O(8)	1.638(6)
Mo(1)-O(10)	1.821(6)	Mo(5)-O(5)#1	1.918(6)
Mo(1)-O(23)#1	2.045(5)	Mo(5)-O(15)#1	1.922(6)
Mo(1)-O(2)	2.071(5)	Mo(5)-O(14)	1.943(6)
Mo(1)-O(19)	2.487(8)	Mo(5)-O(16)	1.944(7)
Mo(1)-O(20)	2.501(9)	Mo(6)-O(11)	1.630(5)
Mo(2)-O(4)	1.654(6)	Mo(6)-O(18)	1.905(6)
Mo(2)-O(5)	1.829(6)	Mo(6)-O(12)	1.909(6)
Mo(2)-O(18)	1.835(6)	Mo(6)-O(17)	1.949(6)
Mo(2)-O(6)	2.044(5)	Mo(6)-O(10)	1.964(7)
Mo(2)-O(23)	2.045(5)	Mo(6)-O(21)	2.510(8)
Mo(2)-O(21)	2.513(10)	Fe(1)-O(1)	2.112(5)
Mo(3)-O(9)	1.661(5)	Fe(1)-N(4)	2.120(6)
Mo(3)-O(15)	1.816(7)	Fe(1)-N(2)	2.127(7)
Mo(3)-O(12)	1.833(6)	Fe(1)-O(1B)	2.158(6)
Mo(3)-O(3)#1	2.035(5)	Fe(1)-N(1)	2.186(7)
Mo(3)-O(2)	2.065(6)	Fe(1)-N(5)	2.229(6)
Mo(3)-O(22)	2.455(9)	V(7)-O(1)	1.638(5)
Mo(4)-O(7)	1.659(5)	V(7)-O(6)	1.919(5)
Mo(4)-O(16)	1.796(7)	V(7)-O(23)	1.924(6)
Mo(4)-O(17)	1.809(7)	V(7)-O(3)	1.929(6)
Mo(4)-O(6)	2.042(6)	V(7)-O(2)#1	1.935(5)
Mo(4)-O(3)	2.064(5)		

Symmetry transformations used to generate equivalent atoms:

#1 -x+1/2, -y+1/2, -z+2

Table S2 The bond angles (°) of main metal atoms for **Fe_2-$PMo_{11}V_3$**.

O(13)-Mo(1)-O(14)	102.7(4)	O(16)-Mo(4)-O(3)	88.8(3)
O(13)-Mo(1)-O(10)	102.0(4)	O(17)-Mo(4)-O(3)	155.3(3)
O(14)-Mo(1)-O(10)	96.0(3)	O(6)-Mo(4)-O(3)	74.1(2)
O(13)-Mo(1)-O(23)#1	100.4(3)	O(7)-Mo(4)-O(21)	157.8(3)
O(14)-Mo(1)-O(23)#1	91.0(2)	O(16)-Mo(4)-O(21)	96.2(4)
O(10)-Mo(1)-O(23)#1	154.3(3)	O(17)-Mo(4)-O(21)	66.0(3)
O(13)-Mo(1)-O(2)	100.0(3)	O(6)-Mo(4)-O(21)	62.7(3)
O(14)-Mo(1)-O(2)	154.9(3)	O(3)-Mo(4)-O(21)	89.4(3)
O(10)-Mo(1)-O(2)	89.4(2)	O(8)-Mo(5)-O(5)#1	103.7(3)
O(23)#1-Mo(1)-O(2)	74.5(2)	O(8)-Mo(5)-O(15)#1	102.8(3)
O(13)-Mo(1)-O(19)	160.0(3)	O(5)#1-Mo(5)-O(15)#1	89.4(3)
O(14)-Mo(1)-O(19)	66.4(3)	O(8)-Mo(5)-O(14)	102.8(3)
O(10)-Mo(1)-O(19)	95.9(3)	O(5)#1-Mo(5)-O(14)	85.8(2)
O(23)#1-Mo(1)-O(19)	64.4(3)	O(15)#1-Mo(5)-O(14)	154.4(4)
O(2)-Mo(1)-O(19)	88.7(3)	O(8)-Mo(5)-O(16)	102.9(4)
O(13)-Mo(1)-O(20)	159.2(3)	O(5)#1-Mo(5)-O(16)	153.4(3)
O(14)-Mo(1)-O(20)	96.4(3)	O(15)#1-Mo(5)-O(16)	86.1(3)
O(10)-Mo(1)-O(20)	67.4(3)	O(14)-Mo(5)-O(16)	87.1(3)
O(23)#1-Mo(1)-O(20)	87.3(3)	O(11)-Mo(6)-O(18)	102.5(4)
O(2)-Mo(1)-O(20)	63.2(3)	O(11)-Mo(6)-O(12)	101.8(3)
O(19)-Mo(1)-O(20)	39.3(3)	O(18)-Mo(6)-O(12)	90.2(3)
O(4)-Mo(2)-O(5)	103.4(3)	O(11)-Mo(6)-O(17)	101.7(4)
O(4)-Mo(2)-O(18)	103.1(4)	O(18)-Mo(6)-O(17)	86.1(3)
O(5)-Mo(2)-O(18)	95.6(3)	O(12)-Mo(6)-O(17)	156.5(3)
O(4)-Mo(2)-O(6)	100.9(3)	O(11)-Mo(6)-O(10)	102.3(3)
O(5)-Mo(2)-O(6)	153.4(3)	O(18)-Mo(6)-O(10)	155.1(3)
O(18)-Mo(2)-O(6)	89.1(2)	O(12)-Mo(6)-O(10)	86.6(3)
O(4)-Mo(2)-O(23)	101.7(3)	O(17)-Mo(6)-O(10)	87.1(3)
O(5)-Mo(2)-O(23)	89.9(2)	O(11)-Mo(6)-O(21)	158.9(3)
O(18)-Mo(2)-O(23)	152.6(3)	O(18)-Mo(6)-O(21)	62.6(3)
O(6)-Mo(2)-O(23)	74.8(2)	O(12)-Mo(6)-O(21)	93.6(3)
O(4)-Mo(2)-O(21)	157.0(3)	O(17)-Mo(6)-O(21)	64.2(3)
O(5)-Mo(2)-O(21)	96.5(3)	O(10)-Mo(6)-O(21)	92.9(3)
O(18)-Mo(2)-O(21)	63.2(3)	O(1)-Fe(1)-N(4)	95.7(2)
O(6)-Mo(2)-O(21)	62.4(3)	O(1)-Fe(1)-N(2)	169.2(3)
O(23)-Mo(2)-O(21)	89.5(3)	N(4)-Fe(1)-N(2)	95.1(3)
O(9)-Mo(3)-O(15)	102.4(3)	O(1)-Fe(1)-O(1B)	87.8(2)
O(9)-Mo(3)-O(12)	102.7(3)	N(4)-Fe(1)-O(1B)	96.4(3)
O(15)-Mo(3)-O(12)	95.6(3)	N(2)-Fe(1)-O(1B)	91.3(3)
O(9)-Mo(3)-O(3)#1	100.0(3)	O(1)-Fe(1)-N(1)	92.5(3)
O(15)-Mo(3)-O(3)#1	90.9(2)	N(4)-Fe(1)-N(1)	166.1(3)
O(12)-Mo(3)-O(3)#1	154.4(3)	N(2)-Fe(1)-N(1)	76.9(3)
O(9)-Mo(3)-O(2)	100.2(3)	O(1B)-Fe(1)-N(1)	95.1(3)

O(15)-Mo(3)-O(2)	155.4(3)	O(1)-Fe(1)-N(5)	95.1(2)
O(12)-Mo(3)-O(2)	88.7(3)	N(4)-Fe(1)-N(5)	76.2(3)
O(3)#1-Mo(3)-O(2)	75.7(2)	N(2)-Fe(1)-N(5)	87.2(3)
O(9)-Mo(3)-O(22)	158.5(3)	O(1B)-Fe(1)-N(5)	172.3(2)
O(15)-Mo(3)-O(22)	65.5(3)	N(1)-Fe(1)-N(5)	91.8(2)
O(12)-Mo(3)-O(22)	96.3(3)	O(1)-V(7)-O(6)	115.4(3)
O(3)#1-Mo(3)-O(22)	64.0(3)	O(1)-V(7)-O(23)	116.1(3)
O(2)-Mo(3)-O(22)	90.0(3)	O(6)-V(7)-O(23)	80.5(2)
O(7)-Mo(4)-O(16)	104.1(4)	O(1)-V(7)-O(3)	111.6(3)
O(7)-Mo(4)-O(17)	102.5(3)	O(6)-V(7)-O(3)	80.0(2)
O(16)-Mo(4)-O(17)	96.4(4)	O(23)-V(7)-O(3)	132.3(3)
O(7)-Mo(4)-O(6)	100.1(3)	O(1)-V(7)-O(2)#1	112.5(3)
O(16)-Mo(4)-O(6)	152.3(3)	O(6)-V(7)-O(2)#1	132.1(3)
O(17)-Mo(4)-O(6)	91.1(3)	O(23)-V(7)-O(2)#1	80.5(2)
O(7)-Mo(4)-O(3)	99.6(3)	O(3)-V(7)-O(2)#1	81.3(2)

Table S3 Hydrogen bonds for **Fe_2-$PMo_{11}V_3$** [Å and °].

D-H···A	D-H	H···A	D···A	D-H···A
N3-H3···O10	0.8600	2.3000	3.025(11)	142.00
N6-H6···O2	0.8600	2.5900	3.395(9)	156.00
C14-H14···O11	0.9300	2.5700	3.254(14)	130.00
C21-H21···O9	0.9300	2.5400	3.194(13)	127.00
C23-H23···O12	0.9300	2.4900	3.332(12)	151.00

Table S4 The BVS results for the Mo, V and Fe ions in **Fe_2-$PMo_{11}V_3$**.

		Bond distance (Å)	BVS calc. for Mo(V)	BVS calc. for Mo(VI)			Bond distance (Å)	BVS calc. for Mo(V)	BVS calc. for Mo(VI)
Mo1(V1)	O(13)	1.655	1.8271	1.9390	Mo4(V4)	O(7)	1.659	1.8074	1.9181
	O(14)	1.809	1.2050	1.2788		O(16)	1.796	1.2481	1.3246
	O(10)	1.821	1.1666	1.2380		O(17)	1.809	1.2050	1.2788
	O(23)#1	2.045	0.6368	0.6758		O(6)	2.042	0.6420	0.6813
	O(2)	2.071	0.5936	0.6299		O(3)	2.064	0.6049	0.6420
	O(19)	2.487	0.1928	0.2046		O(21)	2.500	0.1862	0.1976
	O(20)	2.501	0.1857	0.1970					
Charge			5.8074	6.1632	Charge			5.6935	6.0423
Mo2(V2)	O(4)	1.654	1.8320	1.9442	Mo5(V5)	O(8)	1.638	1.8469	1.9601
	O(5)	1.829	1.1416	1.2115		O(5)#1	1.918	0.9048	0.9603
	O(18)	1.835	1.1232	1.1921		O(15)#1	1.922	0.8903	0.9448
	O(6)	2.044	0.6385	0.6776		O(14)	1.943	0.8389	0.8903
	O(23)	2.045	0.6368	0.6758		O(16)	1.944	0.8366	0.8879
	O(21)	2.513	0.1797	0.1908					
Charge			5.5518	5.8920	Charge			5.3175	5.6433
Mo3(V3)	O(9)	1.661	1.7977	1.9078	Mo6(V6)	O(11)	1.630	1.9548	2.0745

	O(15)	1.816	1.1824	1.2549		O(18)	1.905	0.9296	0.9866
	O(12)	1.833	1.1293	1.1985		O(12)	1.909	0.9196	0.9760
	O(3)#1	2.035	0.6542	0.6943		O(17)	1.949	0.8254	0.8760
	O(2)	2.065	0.6033	0.6402		O(10)	1.964	0.7926	0.8412
	O(22)	2.455	0.2102	0.2231		O(21)	2.510	0.1812	0.1923
Charge			5.5771	5.9188	Charge			5.6032	5.9465

The calculated value of average oxidation state of Mo: 5.890

The theoretical value of average oxidation state of Mo: 5.880

		Bond distance (Å)	BVS calc. for V(III)	BVS calc. for V(IV)	BVS calc. for V(V)
V1(Mo1)	O(13)	1.655	1.2892	1.4019	1.4918
	O(14)	1.809	0.8503	0.9246	0.9839
	O(10)	1.821	0.8232	0.8951	0.9525
	O(23)#1	2.045	0.4493	0.4886	0.5199
	O(2)	2.071	0.4188	0.4554	0.4847
	O(19)	2.487	0.1361	0.1480	0.1574
	O(20)	2.501	0.1310	0.1425	0.1516
Charge			3.9669	4.3136	4.5903
V2(Mo2)	O(4)	1.654	1.2927	1.4057	1.4959
	O(5)	1.829	0.8056	0.8760	0.9321
	O(18)	1.835	0.7926	0.8619	0.9171
	O(6)	2.044	0.4505	0.4899	0.5213
	O(23)	2.045	0.4493	0.4886	0.5199
	O(21)	2.513	0.1268	0.1379	0.1468
Charge			3.9176	4.2600	4.5332
V3(Mo3)	O(9)	1.661	1.2685	1.3794	1.4678
	O(15)	1.816	0.8344	0.9073	0.9655
	O(12)	1.833	0.7969	0.8665	0.9221
	O(3)#1	2.035	0.4616	0.5020	0.5342
	O(2)	2.065	0.4257	0.4629	0.4926
	O(22)	2.455	0.1484	0.1613	0.1717
Charge			3.9355	4.2794	4.5538
V4(Mo4)	O(7)	1.659	1.2754	1.3868	1.4758
	O(16)	1.796	0.8807	0.9577	1.0191
	O(17)	1.809	0.8503	0.9246	0.9839
	O(6)	2.042	0.4530	0.4926	0.5242
	O(3)	2.064	0.4268	0.4338	0.4939
	O(21)	2.500	0.1314	0.1429	0.1520
Charge			4.0176	4.3384	4.6489
V5(Mo5)	O(8)	1.638	1.3499	1.4678	1.5620
	O(5)#1	1.918	0.6333	0.6887	0.7329
	O(15)#1	1.922	0.6265	0.6813	0.7250
	O(14)	1.943	0.5920	0.6437	0.6850

	O(16)	1.944	0.5904	0.6420	0.6831
Charge			3.7920	4.1234	4.3879
V6(Mo6)	O(11)	1.630	1.3794	1.4999	1.5961
	O(18)	1.905	0.6560	0.7133	0.7591
	O(12)	1.909	0.6489	0.7056	0.7509
	O(17)	1.949	0.5824	0.6333	0.6740
	O(10)	1.964	0.5593	0.6082	0.6472
	O(21)	2.510	0.1279	0.1390	0.1480
Charge			3.9539	4.2994	4.5752
V7	O(1)	1.638	1.3499	1.4678	1.5620
	O(6)	1.919	0.6316	0.6868	0.7309
	O(23)	1.924	0.6231	0.6776	0.7211
	O(3)	1.929	0.6148	0.6685	0.7114
	O(2)#1	1.935	0.6049	0.6578	0.6999
Charge			3.8243	4.1585	4.4252

		Bond distance (Å)	BVS calc. for Fe(II)	BVS calc. for Fe(III)
Fe1	O(1)	2.112	0.3600	0.3852
	N(4)	2.120	0.4280	0.4385
	N(2)	2.127	0.4200	0.4303
	O(1B)	2.158	0.3179	0.3401
	N(1)	2.186	0.3581	0.3669
	N(5)	2.229	0.2624	0.2808
Charge			2.1464	2.2418

Table S5 The Mo/V ratios of Mo1/V1-Mo6/V6 in **Fe_2-$PMo_{11}V_3$**.

Ratio	Mo	V
Mo1/V1	0.96	0.04
Mo2/V2	0.94	0.06
Mo3/V3	0.94	0.06
Mo4/V4	0.94	0.06
Mo5/V5	0.84	0.16
Mo6/V6	0.83	0.17

Table S6 Nitrogen sorption results of **Fe_2-$PMo_{11}V_3$**.

Catalyst	A_{BET} (m^2/g)	Pore volume (cm^3/g)	Average pore diameter (nm)
Fe_2-$PMo_{11}V_3$	8.856	0.050	22.794

References

1. J. An, Y. Wang, W. Dong, X. Gao, O. Yang, Y. Liu, J. Zhao and D. Li, *ACS Appl. Energy Mater.* 2022, **5**, 2384-2390.
2. I. Tamiolakis, I.N. Lykakis, A.P. Katsoulidis, M. Stratakis and G.S. Armatas, *Chem. Mater.* 2011, **23**, 4204-4211.
3. L. Zhou, L. Wang, S. Zhang, R. Yan and Y. Diao, *J. Catal.* 2015, **329**, 431-440.